2730–2743 *Nucleic Acids Research, 2015, Vol. 43, No. 5* *Published online 26 February 2015*
doi: 10.1093/nar/gkv146

Dynamic *Escherichia coli* SeqA complexes organize the newly replicated DNA at a considerable distance from the replisome

Emily Helgesen[1,†], Solveig Fossum-Raunehaug[1,2,†], Frank Sætre[1], Kay Oliver Schink[3] and Kirsten Skarstad[1,2,*]

[1]Department of Cell Biology, Institute for Cancer Research, Oslo University Hospital, Radiumhospitalet, 0310 Oslo, Norway, [2]School of Pharmacy, Faculty of Mathematics and Natural Sciences, University of Oslo, 0316 Oslo, Norway and [3]Department of Biochemistry, Institute for Cancer Research, Oslo University Hospital, Radiumhospitalet, 0310 Oslo, Norway

Received November 12, 2014; Revised February 12, 2015; Accepted February 14, 2015

ABSTRACT

The *Escherichia coli* SeqA protein binds to newly replicated, hemimethylated DNA behind replication forks and forms structures consisting of several hundred SeqA molecules bound to about 100 kb of DNA. It has been suggested that SeqA structures either direct the new sister DNA molecules away from each other or constitute a spacer that keeps the sisters together. We have developed an image analysis script that automatically measures the distance between neighboring foci in cells. Using this tool as well as direct stochastic optical reconstruction microscopy (dSTORM) we find that in cells with fluorescently tagged SeqA and replisome the sister SeqA structures were situated close together (less than about 30 nm apart) and relatively far from the replisome (on average 200–300 nm). The results support the idea that newly replicated sister molecules are kept together behind the fork and suggest the existence of a stretch of DNA between the replisome and SeqA which enjoys added stabilization. This could be important in facilitating DNA transactions such as recombination, mismatch repair and topoisomerase activity. In slowly growing cells without ongoing replication forks the SeqA protein was found to reside at the fully methylated origins prior to initiation of replication.

INTRODUCTION

The cell cycle of all living organisms involves the precisely coordinated events of chromosome replication, segregation and cell division. In order to ensure genetic stability, the genetic material must be correctly replicated once per cell cycle and properly organized and segregated to the new daughter cells. *Escherichia coli* cells are capable of replicating with overlapping replication cycles during rapid growth (1). This means that new DNA is constantly being synthesized and that the circular chromosome may have more than two replication forks. Unlike in eukaryotic cells replication and segregation of DNA is not separated in time. How the cells ensure proper organization and partitioning of DNA at the same time as replication, transcription, recombination and repair processes are going on is not fully understood. Many DNA binding proteins, so-called NAPs (nucleoid associated proteins), have been implicated in the process (2). Among them is the SeqA protein that preferentially binds to newly replicated DNA.

SeqA was initially discovered as an actor in origin sequestration (3) that prevents re-initiation of replication at new origins for about 1/3 of the cell cycle (3–5). The binding of SeqA to DNA *in vitro* requires at least two hemimethylated (newly replicated) GATC sites that are appropriately spaced (6), whereas if the DNA is fully methylated only *oriC* DNA (which has a very high frequency of GATC sites) can bind SeqA (7). If more than six hemimethylated GATC sites are present on a DNA fragment the resulting oligomer of SeqA is capable of recruiting further SeqA molecules that need not be bound to DNA (8). It has also been shown that SeqA is capable of restraining negative supercoils (9–11) by forming multimer fibers (11,12). The *in vitro* work indicates that large structures of SeqA trail the replication forks. This is supported *in vivo* by fluorescence microscopy studies showing that SeqA colocalizes with BrdU labeled, newly synthesized DNA (13,14) and forms a relatively compact structure (15,16). This structure must at the same time be dynamic, since SeqA continuously binds the newest (most

*To whom correspondence should be addressed. Tel: +47 22781982; Fax: +47 22781995; Email: kirsten.skarstad@labmed.uio.no
†These authors contributed equally to the paper as first authors.
Present address: Frank Sætre, Prostate Cancer Research Group, Centre for Molecular Medicine, University of Oslo, 0318 Oslo, Norway.

recently replicated) DNA (17). Chromatin immunoprecipitation (ChIP) on chip analysis highlights that the binding of SeqA on the chromosome correlates with hemimethylation (18) and recent high-resolution genome conformation capture analysis showed replication-dependent clustering of SeqA-binding sequences and suggested an important role for SeqA in organization of the chromosome during replication (19).

Two models for the role of SeqA-mediated DNA organization behind the replication fork have been proposed. The first is that SeqA complexes direct segregation of the sister chromosomes during replication by keeping sister DNA molecules separate from each other and from the replication forks (20). The second model is that the SeqA complexes constitute a spacer in which sister DNA molecules are kept close together. Such a function could keep segregation from destabilizing the replication fork (21,22). The model is supported by the fact that SeqA deletion strains have compromised genomic stability (3,23) and more rapid DNA segregation (24) compared to wild-type strains. The SeqA protein has also been shown to interact with TopoIV (25). On newly replicated DNA this interaction may facilitate removal of precatenanes and subsequent chromosome segregation (24).

Here we have studied the relative positions of the replisome and SeqA structures with fluorescence microscopy during rapid growth with overlapping replication cycles and during slow growth with only one replicating chromosome. We find that the SeqA structures bound to newly formed, hemimethylated sister DNA molecules are situated close together (closer than ∼30 nm) but at a considerable distance behind the replisome (on average ∼200–300 nm).

MATERIALS AND METHODS

Bacterial strains

All strains used in experiments are derivatives of the *E. coli* K-12 strain AB1157 (26) and are listed in Table 1. Localization studies of SeqA were done with cells containing the yellow fluorescent protein (YFP) fused to the C-terminal end of SeqA. The *seqA-yfp* gene was expressed from the endogenous chromosomal promoter. The YFP protein was from (27) and connected to SeqA via a four-amino acid linker (28). SeqA-YFP was transferred into AB1157 by P1 transduction (29) to obtain SF128. The SeqA-YFP fusion is functional in origin sequestration and western blot analysis showed that the cellular concentration of fluorescently tagged SeqA was about the same as that of wild-type SeqA (30).

A FROS (fluorescent-repressor-operator system) was used to study the localization of the origin region (31). The RRL215 strain contained a *lac* operator array (240 copies) (from IL01) (31,32) and a *lacI-mcherry* gene (33). The *lac* operator array was located at the *att*Tn7 site (at 84.27 min) 15 kb counterclockwise from *oriC*. The *lacI-mcherry* gene replaced the *leuB* gene on the chromosome and was constitutively expressed from the *dnaA* promoter (Table 1). The strain was kindly provided by R. Reyes-Lamothe and D.J. Sherratt. For multiple insertions of modified genes, the chloramphenicol resistance gene with flanking flip recognition target (*frt*) sites was removed from RRL215 and SF128 with the aid of Flp recombinase from pCP20 (34) to yield strains SF143 and SF144, respectively (Table 1). To obtain strain SF148, *seqA-yfp* (from SF128) was P1 transduced (29) into SF143 cells. Studies of SSB localization were with cells containing the SSB-CFP allele inserted in place of the *E. coli lamB* gene and was kindly provided by A Wright (G. Leung *et al.*, unpublished). To obtain SF149 and SF171, an *ssb-cfp* fusion (from GL224) was P1 transduced into SF144 (this work) and RRL27 (33), respectively. The SF149 and SF171 cells contained the wild-type *ssb* gene on the chromosome.

Cell growth

Cells were grown at 28°C in AB minimal medium (35) supplemented with 1-μg ml^{-1} thiamine, 0.2% glucose and 0.5% casamino acids (glucose-CAA medium) or in AB minimal medium (35) supplemented with 0.4% sodium acetate, 1-μg ml^{-1} thiamine, 80-μg ml^{-1} threonine, 20-μg ml^{-1} leucine, 30-μg ml^{-1} proline, 22-μg ml^{-1} histidine and 22-μg ml^{-1} arginine (acetate medium). The doubling time (τ) was found by optical density (OD) measurements. Cells were grown to OD ∼ 0.15 (early exponential phase) at which time they were prepared for flow cytometry analysis or fluorescence microscopy.

Flow cytometry and cell cycle analysis

Exponentially growing cells were fixed in ethanol or treated with 300-μg/m rifampicin and 10-μg/ml cephalexin to inhibit replication initiation (36) and cell division (37), respectively. Growth of drug-treated samples continued for 3–4 generations, after which they were fixed in ethanol. Drug-treated cells ended up with an integral number of chromosomes (36), which represents the number of origins at the time of drug treatment (replication run-out). Run-out samples were only prepared for cells grown in glucose-CAA medium due to rifampicin resistant initiations during growth in acetate medium (38). Flow cytometry was performed as previously described (39) using an LSR II flow cytometer (BD Biosciences) and FlowJo 7.2.5 software. Cell cycle parameters, numbers of origins and replication forks per cell were obtained by analysis of the DNA distributions obtained by flow cytometry as described (40) (see Supplementary Figures S1 and S2).

Widefield fluorescence microscopy imaging

For widefield fluorescence microscopy exponentially growing cells were immobilized on an agarose pad (1% agarose in phosphate-buffered saline) and covered with a #1.5 coverslip. Images were acquired with a Leica DM6000 microscope equipped with a Leica EL6000 metal halide lamp and a Leica DFC350 FX monochrome CCD camera. Phase contrast imaging was performed with an HCX PLAPO 100x/1.40 NA objective, whereas differential interference contrast images were acquired with an HCX PL APO 100x/1.46 NA objective. Narrow band-pass filter sets (CFP: Ex BP436/20, Em BP480/40, GFP: Ex BP470/40, Em BP525/50, YFP: Ex BP510/20, Em BP560/40, Cy3: Ex BP545/30, Em BP610/75) were used for fluorescence imaging.

Table 1. Bacterial strains

Strain name	Relevant features[a]	Source
AB1157	Wild type	(26)
MG1655 *seqA-YFP*	MG1655 *seqA-yfp::cat*	(28)
GL224	MG1655 *SSB-CFP::cat* in *lamB*	A. Wright and G. Leung
RRL27	AB1157 *holC-ypet::kan*	(33)
RRL215[b]	AB1157 *ori1* [lacO240-Hyg]3908 P*dnaA-lacI-mcherry cat*::D*leuB*	R. Reyes-Lamothe and D.J. Sherratt
SF128	AB1157 *seqA- yfp::cat*	(30)
SF143	RRL215 with *cat* flipped out	This work
SF144	SF128 with *cat* flipped out	This work
SF148	AB1157 *ori1* [lacO240-*hyg*]3908 P*dnaA-lacI-mcherry seqA-yfp::cat*	This work
SF149	AB1157 *seqA-yfp SSB-CFP::cat*	This work
SF171	AB1157 *holC-ypet::kan SSB-CFP::cat*	This work

[a]For the description of strain constructions see the Materials and Methods section.
[b]The construction of strain RRL215 was performed as described in (33) except that the lac promoter was substituted with the dnaA promoters (R. Reyes-Lamothe personal communication). The primers used for up-amplification of the dnaA promoters were as follows:
PdnaA-F (PciI, ACATGT) 5′-GTC ACA TGT AAT AAT TGT ACA CTC CG-3′
PdnaA-R (EcoRI, GAATTC) 5′-AAG AAT TCT CCA CTC GAA CAA AAG TCG-3′

During image acquisition, saturated pixels were avoided. The raw images were saved for further image processing (see below and Supplementary materials).

Single-molecule localization microscopy by dSTORM imaging

dSTORM (direct stochastic optical reconstruction microscopy) imaging was performed using an OMX V4 system (Applied Precision, a GE Healthcare company). Fixed cells (from exponential growth) were mounted on poly-L-lysine-coated Mattec dishes and stained with rabbit anti-SeqA primary antibody and anti-rabbit Alexa647 secondary antibody, according to the protocol described in (41). The cells were imaged in switching buffer (50-mM Tris, 50-mM NaCl, 10% Glucose, 2000-Units/ml Catalase, 270-U/ml Glucose Oxidase and 147-mM beta-Mercaptoethanol) (42).

Five-thousand frames per field of view were recorded in TIRF (Total Internal Reflection Fluorescence) imaging mode using a 100-mW 642 laser line.

All single-molecule reconstructions were performed using Softworx software (Applied Precision, a GE Healthcare company). Molecules were localized using multi-emitter fitting and drift was corrected by cross correlation. For final visualization, we plotted only molecules with 5–15-nm localization precision with 10-nm final pixel size.

Image processing and analysis

For all microscope techniques, imaging adjustments (brightness and contrast) were performed in Image J, Fiji or Adobe Photoshop CS4 software. We used the public domain Coli-Inspector project to obtain fluorescence intensity profiles of the cells and to do vertical plotting of fluorescence and phase contrast images of cells. Coli-Inspector runs under ImageJ/Fiji in combination with the plugin ObjectJ (http://simon.bio.uva.nl/objectj/). The average fluorescence intensity profile of cells was plotted against the cell long axis, in groups of increasing cell length, as described (43). Vertical plotting of cells was done in the order of gradual increase in cell length. Age classes of cells were defined by the cell length, assuming that length increases linearly.

Image processing for automated analysis using the developed script (see below) was performed in Image J using the following tools: (i) background subtraction with default Rolling disk (diameter 10 pixels), (ii) deconvolution using the Richardson—Lucy algorithm (100 iterations), (iii) median filter, (iv) thresholding by Max Entropy (see Supplementary Figure S5 and Supplementary materials for details of image processing).

Analysis of fluorescence spot distances, colocalization and numbers of foci per cell

We have developed a Python-based script for automatic measurements of the distance between neighboring spots that are registered in two different fluorescence channels. The script is run under Fiji and uses ‘Find Maxima’ as a tool for spot/focus detection within the specimen. The measured distances were also used to estimate the level of colocalization (object-based colocalization) (see Supplementary materials). The script was evaluated by analysis of fluorescently labeled TetraSpeck beads and cells with fluorescently tagged replisome proteins (SSB and HolC) and found to work well (see Supplementary materials).

The numbers of fluorescent foci per cell were counted manually or by using the script. We found that the distribution of numbers of foci was essentially the same when using these two methods (data not shown).

Investigations of distortions in the image plane

To investigate distortions in the image plane, an Image Registration Target Slide (Applied Precision) was employed (see Supplementary materials). We found that the light path of the microscope system was properly aligned for colocalization studies (Supplementary Figure S4).

RESULTS

The SeqA structure trails the replication fork with an average distance of 212 nm in rapidly growing cells

Using widefield fluorescence imaging (snapshot imaging) we have simultaneously visualized the replisome (SSB-CFP) and the SeqA protein (SeqA-YFP) in *E. coli* SF149 cells in order to investigate their relative localizations. In agreement with (33) we find that SSB is a good marker of the replisome because the positions of SSB foci are coincident with those of the replisome component HolC (Supplementary Figure S3).

The cells were grown at 28°C in minimal medium supplemented with glucose and casamino acids (glucose-CAA medium) (doubling time (τ) of 57 ± 1 min) to early exponential phase (OD ∼ 0.15) and samples were prepared for microscopy or flow cytometry analysis. Cell cycle analysis of DNA histograms of cells growing exponentially or treated with rifampicin and cephalexin to allow run-out of replication (see the Materials and Methods section) showed that initiation of replication occurred at four origins at the age of ∼0.8 and terminated right before cell division in the following generation (overlapping replication). The cells contained two replication forks per chromosome (in total four forks in young cells and eight forks in dividing cells), except for in the period after initiation and prior to termination where each of the two chromosomes contained six replication forks (multifork replication) (Figure 1A and Supplementary Figure S1). Snapshot imaging showed formation of mainly two, three or four discrete SeqA and replisome foci (Figure 1B and E). The distribution of SeqA foci is in accordance with previous immunofluorescence results (16) and indicates that pairs of replication forks are situated close together for most of the cell cycle. The public domain Coli-Inspector project (see the Materials and Methods section) was used to visualize the trend of SeqA focus movement through the cell cycle (Figure 1C and D). Note that Figure 1A, B and C are aligned according to relative cell age (newborn cells represented in top panels and dividing cells in bottom panels). The youngest/newborn cells mainly had one SeqA focus and one replisome focus at each of the quarter positions. Since these cells contained four replication forks, the two replication forks of each chromosome must be localized close together, as mentioned above (Figure 1B, top panel). SeqA and replisome foci could be distinguished as four separate foci when the replication forks had replicated more than half of the chromosome, around the age of 0.3–0.45 (i.e. one SeqA/replisome focus per replication fork) (Figure 1B, panel 3). Splitting of paired replication forks has been observed in previous studies at this stage in the replication cycle (30), and indicates that a movement of the DNA takes place. Using 3D-SIM (three-dimensional structured illumination microscopy) with a resolution of ∼120 nm we found that the two SeqA structures trailing a replication fork also could be resolved in a few cells in this period (∼6% of the total population) (Supplementary Figure S6). It therefore appears likely that not only the replication forks are more dynamic/mobile relative to each other in this period, but also the individual strands of newly replicated DNA. However, in ages of ∼0.45–0.8 (prior to and at initiation of a new round of replication) pairs of replication forks were once again found to be colocalized (two SeqA/replisome foci in each cell), presumably because the replication forks are converging toward the terminus region of the chromosome. After initiation (age 0.8–1), the cells mainly harbored four foci positioned at the cells one-eighth positions (Figure 1B, lower panels). In this period the cells contained four chromosomes, which means that each focus likely represents a pair of new replication forks each. Some of the cells in this age group (presumably those with 12 replication forks) contained six replisome foci but only four SeqA foci (Figure 1B, panels 5 and 6). This was about 10% of the population, and in these cases, the 'old' forks might have lost the SeqA structures trailing them due to few GATC sites in the Ter domain, as suggested previously (18).

As seen from snap shot images the replisome and SeqA foci were near each other and had similar localization patterns, but only occasionally cells contained completely overlapping SeqA and replisome foci (Figure 1B). This indicated that the dynamic SeqA structures on the new DNA are trailing the replication forks, but do not bind immediately behind them. To quantitatively assess the distance between SeqA and replisome structures we developed a Python-based image analysis script. The script is run under Fiji and uses 'Find Maxima' as a tool for detecting the center-of-mass of the fluorescent foci in two separate channels. It calculates the distance between nearest-neighbor foci in the two channels, in our case between SeqA and the replisome (see Supplementary materials). Because the foci are registered in separate channels, it is possible to determine distances that are below the resolution limit of the microscope (see Supplementary materials). Using this analysis method we found that the average SeqA-replisome distance was 212 ± 15 nm (average ± SEM). The cells were further divided into five age groups based on increasing cell length and the distribution of SeqA-replisome distances within each age group was plotted in a histogram (color coded distance categories), as well as the average distance for each group (red text above the histograms) (Figure 1F). The analysis showed that the SeqA-replisome distances were relatively similar through the cell cycle (Figure 1F). Thus, our results indicate that the SeqA protein is trailing the replisome at a considerable distance of on average 212 nm through the cell cycle in rapidly growing cells.

The SeqA structure trails the replication fork at a considerable distance also in slowly growing cells

Slowly growing cells with a maximum of two replication forks and a period devoid of replication were also analyzed. This was done in order to simplify the interpretation of foci in the images (no multifork system) and to investigate whether the SeqA-replisome distances would differ between rapid and slow growth conditions. The cells (SF149) were grown at 28°C in minimal medium supplemented with acetate (acetate medium) (τ = 203 ± 3 min) to early exponential phase (OD ∼ 0.15). Snapshot imaging and flow cytometry analysis was performed as described above. Cell cycle analysis showed that initiation of replication occurred at one origin in the newborn cell and that the replication pe-

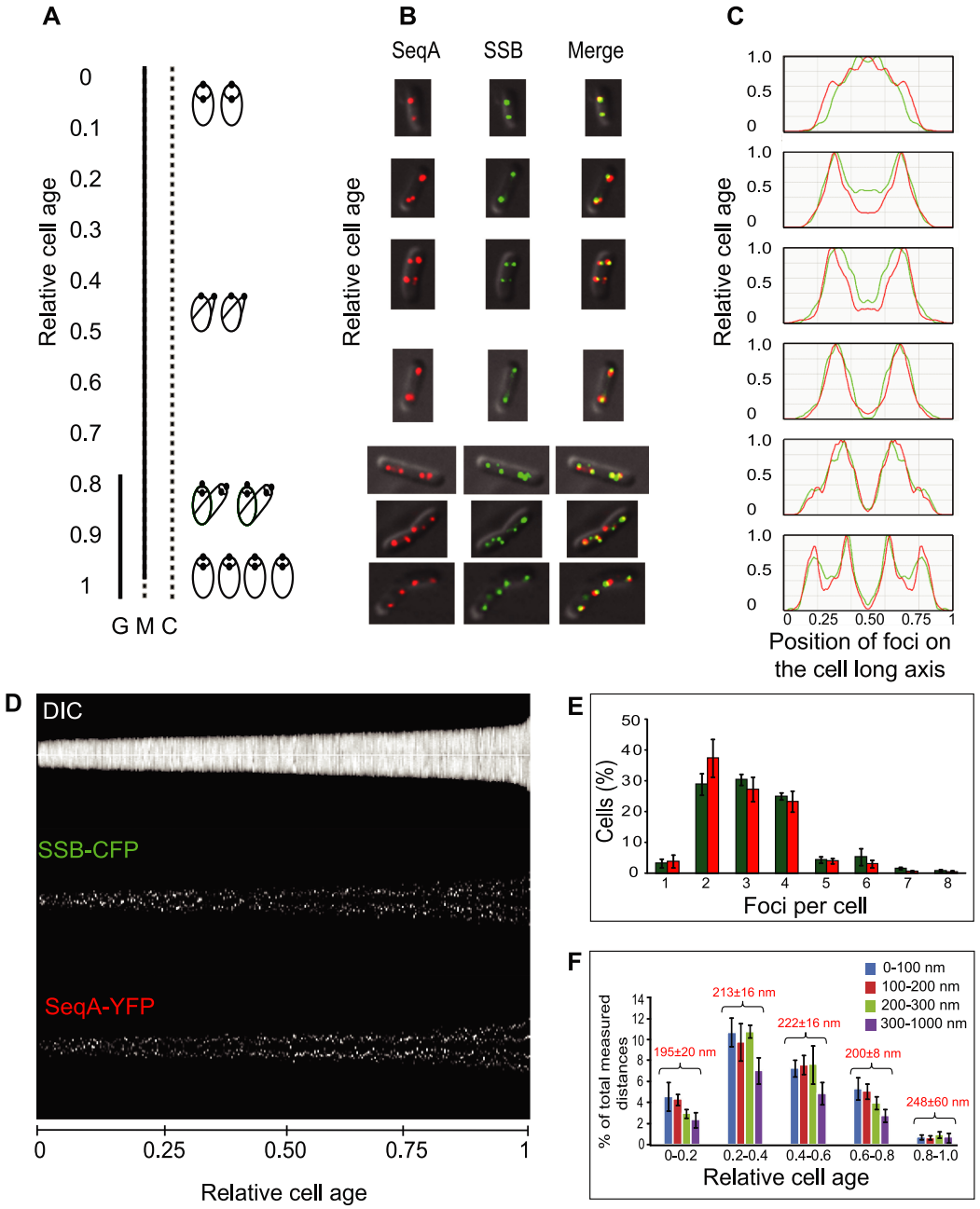

Figure 1. Snapshot imaging of cells with fluorescently tagged SeqA and replisome during rapid growth in glucose-CAA medium. (**A**) Cell cycle diagram with parameters obtained by flow cytometry of cells (SF149) with tagged SeqA (SeqA-YFP) and replisome (SSB-CFP), grown exponentially in glucose-CAA medium at 28°C. The relative cell age is indicated (from 0 to 1), the C-period (replication period) as a black line and the D-period (period from replication termination to cell division) as a stippled black line. Schematic drawings of replicating chromosomes at different stages of the cell cycle are shown beside the diagram. These indicate DNA content, the number of origins (black dots), the number of replication forks and replication fork progression. G, M and C stand for grand-mother, mother and current generation, respectively. (**B**) Snapshot fluorescence imaging showed formation of discrete SeqA (pseudo-colored red) and replisome (pseudo-colored green) foci. Images of cells are ordered from top to bottom according to relative cell age (based on relative cell length). (**C**) Local brightness of fluorescent replisome (green line) and SeqA (red line) signals was plotted against foci positioning on the cell long axis (x-axis of histograms) using Coli-Inspector (see the Materials and Methods section). The population was divided into six age groups based on relative cell length. The histograms of age groups are vertically plotted according to increasing cell age (youngest cells in the top panel and oldest cells in the bottom panel). (**D**) The integral fluorescence of each cell was sorted and plotted as a function of cell length (each cell is displayed as a vertical line) using Coli-Inspector, where relative cell length corresponds to relative cell age (x-axis). The white horizontal line indicates midcell. A total of 303 cells were analyzed. (**E**) The percentages of cells with zero to seven SeqA (red bars) or replisome (green bars) foci per cell were manually counted (see Supplementary materials) and plotted in a histogram. A total of 281 cells were analyzed. (**F**) The imaged population of cells was divided into five age groups and the distribution of SeqA-replisome distances was plotted in a histogram. The SeqA-replisome distances within each age group were categorized into 0.1-μm intervals represented with color codes (blue category represents distances of 0–100 nm, red category represents distances of 100–200 nm, green category represents distances of 200–300 nm and purple category represents distances of 300–1000 nm). The average SeqA-replisome distances (±SEM) for all cells within each age group are shown above the histograms in red text. The y-axis shows the percentage of total measured SeqA-replisome distances (the distances within categories were normalized against the total number of measured distances for all age groups). A total of 522 cells were analyzed.

riod (C-period) spanned about half a doubling time (Figure 2A and Supplementary Figure S2).

Snapshot fluorescence imaging showed formation of discrete SeqA and replisome foci in ∼90 and 50% of the population, respectively (Figure 2B and E). The newborn cells in the population contained one SeqA and one replisome focus that were localized near each other at midcell (Figure 2B, top panel). This indicates that the two replication forks are situated close together. The replisome was next observed at the quarter positions (in ∼25% of the replicating cells), while SeqA remained at midcell (Figure 2B, purple square). However, the midcell SeqA focus could sometimes be distinguished as two very closely spaced foci. Toward the end of the replication period (ages of ∼0.35–0.45), both SeqA and the replisome were located at midcell (Figure 2B, panel 4). In the post-replication period (D-period) most cells did not contain replisome foci and SSB-CFP was seen as a background haze. SeqA, however, persisted as a focus at midcell for a significant period before relocating to the quarter positions just before cell division (around the relative age of 0.8) (Figure 2B, panels 5 and 6). A few of the non-replicating cells contained three SeqA foci (Figure 2E), usually localized at midcell and quarter positions. We plotted the mean intensity of SeqA foci in the population (estimated for a 5 × 5 pixel around each focus) and found that it correlates inversely with the number of foci in the cell (Supplementary Figure S7). This strengthens the argument that SeqA structures behind two forks are colocalized in cells containing one SeqA focus. The localization patterns of SeqA and replisome foci in the whole population are shown using Coli-Inspector as previously explained (Figure 2C and D).

We employed our script for quantitative analysis of distances between SeqA and replisome foci. The average SeqA-replisome distance for the total population was found to be 256 ± 41 nm, which is relatively similar to that of rapidly growing cells. However, as the images in Figure 2B indicate, the distances vary through the cell cycle and an average distance estimation may not be appropriate. We divided cells of ages 0–0.6 into three groups based on increasing cell length, as explained for Figure 1F (Figure 2F). In the youngest group (age 0–0.2) when initiation occurs most cells had short SeqA-replisome distances (the blue and red distance categories are high and the average distance is 206 ± 8 nm). In the middle group (age 0.2–0.4) it can clearly be seen that the distances between SeqA and the replisome increase (the purple distance category is high and the average distance is 300 ± 47 nm). This is presumably due to the presence of cells with replisomes at the quarter positions and SeqA at midcell (Figure 2B, purple square). The last group (ages of 0.4–0.6) includes cells that are terminating replication, and gives a somewhat decreased average distance (265 ± 59 nm) compared to the middle group. Here the replisomes in many cells were found back at the midcell position (Figure 2B). Thus, these results coincide well with qualitative observations from fluorescence microscopy images (Figure 2B) and show that the distance between SeqA and the replisome can be surprisingly large during certain parts of the cell cycle in slowly growing cells (Figure 2B (purple square) and F).

SeqA-YFP is localized at midcell for most of the D-period, but colocalizes with the origin region before cell division and initiation of replication

We found that during slow growth in acetate medium, fluorescent SeqA foci were present in ∼90% of the cells (Figure 2). Since DNA replication was terminated about halfway through the cell cycle, a substantial part of the population was non-replicating cells with two fully replicated chromosomes. We found that discrete SeqA foci were present in these cells (Figure 2B, C and D, ages of 0.45–1). The GATC sites on the chromosome are targets for DNA adenine methyltransferase that methylates the adenine residues shortly after passage of the replication fork (44). This means that the chromosomes will be fully methylated when replication is finished. Biochemical analysis has shown that SeqA binds preferentially to two or more hemimethylated GATC sites, but is also able to bind fully methylated *oriC* (6,7,45). We therefore speculated whether the SeqA foci observed in the D-period could represent SeqA bound to fully methylated *oriC*. In order to answer this question, we simultaneously visualized the SeqA protein and the *oriC* region using snapshot imaging. The cells (SF148) expressed YFP-tagged SeqA protein and had their *oriC* region marked with fluorescent *lacI* repressor (LacI-mCherry) bound to an array of *lac* operators 15 kb counterclockwise of *oriC*.

The cells were grown at 28°C in acetate medium ($\tau = 242 \pm 25$ min) and samples for flow cytometry and snapshot imaging were prepared as described previously. Initiation of replication occurred at one origin at a relative cell age of ∼0.1 and the replication period (C-period) lasted ∼40% of the doubling time (Figure 3A and Supplementary Figure S2). In accordance with results from Figure 2, snapshot imaging showed formation of discrete SeqA foci in ∼95% of the cells (Figure 3B and E). Discrete origin foci were observed in all cells (Figure 3B and E).

SeqA and origin foci were colocalized at midcell in the youngest/newborn cells (Figure 3B, top panel). In cells with age around 0.2–0.4 the origin region had moved toward the quarter positions, whereas SeqA remained at midcell (Figure 3B, panel 2). In the larger cells, in which the DNA replication was terminated, we observed one SeqA focus at midcell and one origin focus at each of the quarter positions (ages of ∼0.55–0.8) (Figure 3B, panels 4 and 5). Finally, in the old/dividing cells SeqA was colocalized with the origin region at the quarter positions (ages of ∼0.8–1) (Figure 3B, panel 6). Analysis of SeqA and origin localization patterns in the cell was performed with Coli-Inspector as previously explained (Figure 3C and D).

To analyze the distances between SeqA and origin region we employed the script. By dividing the cells into four age groups, we found that the youngest (0–0.2) and the oldest (0.6–1) cells contained the highest fraction of SeqA foci colocalized with the origin region (Figure 3F). In the age groups between, there were substantially less cells with origin proximal SeqA foci. This corresponds well to what we have described above. The high fraction of cells with colocalization of SeqA and the origin region in young cells is in accordance with replication initiation, while the decrease of such cells in middle age groups reflects segregation of the

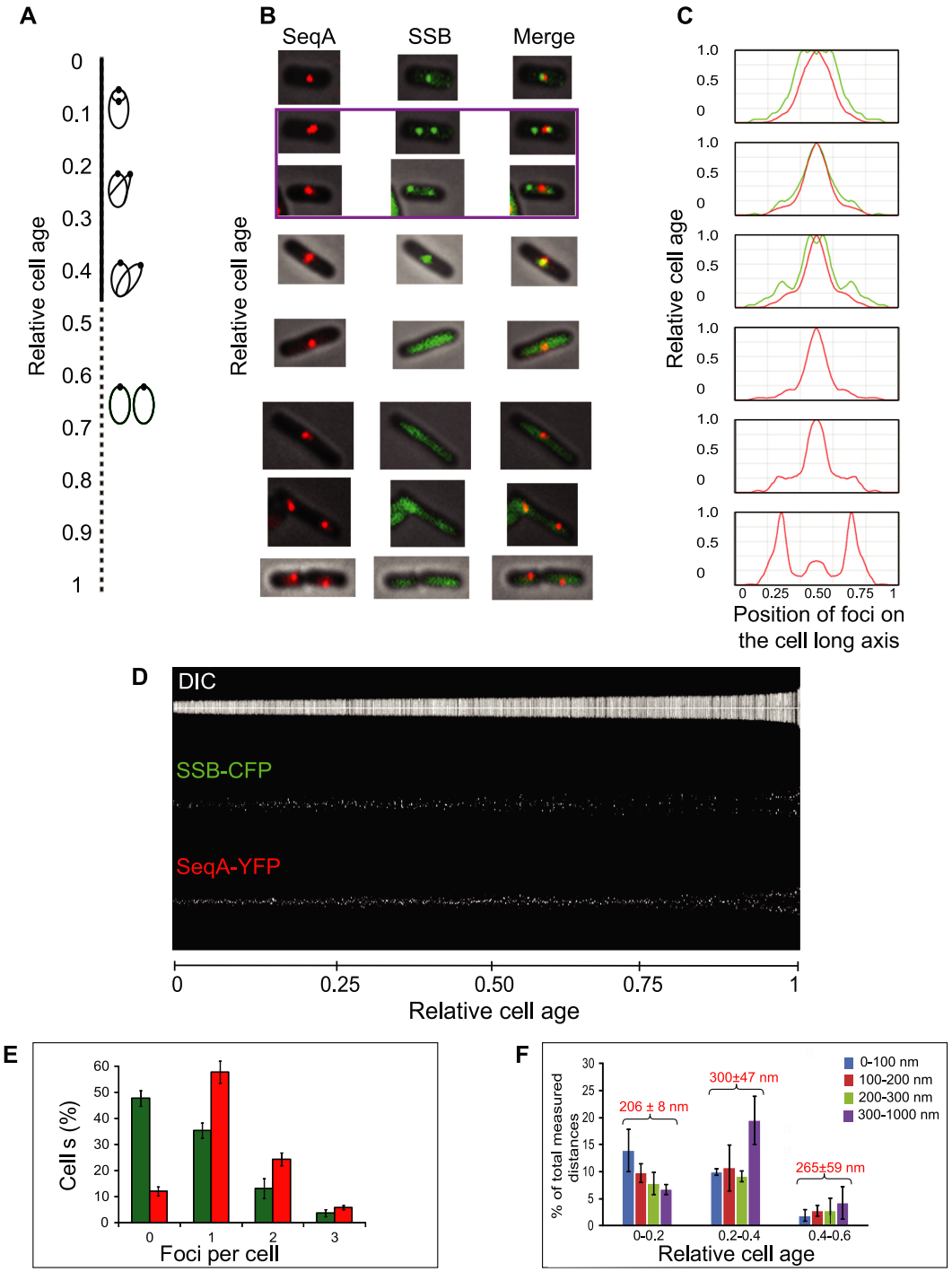

Figure 2. Snapshot imaging of cells with fluorescently tagged SeqA and replisome during slow growth in acetate medium. (**A**) Cell cycle diagram with parameters obtained by flow cytometry of cells (SF149), with tagged SeqA (SeqA-YFP) and replisome (SSB-CFP), grown exponentially in acetate medium at 28°C. See Figure 1A for the description of cell cycle diagram. (**B**) Snapshot fluorescence imaging showed formation of discrete SeqA (pseudo-colored red) and replisome (pseudo-colored green) foci. Images of cells are ordered from top to bottom according to relative cell age (based on relative cell length). The purple square indicates cells in which SeqA was localized at midcell, whereas the replisome was positioned at the quarter positions. (**C**) Local brightness of fluorescent replisome (green line) and SeqA (red line) signals was plotted against foci positioning on the cell long axis (x-axis of histograms) using Coli-Inspector (see the Materials and Methods section). The population was divided into six age groups based on relative cell length. The histograms of age groups are vertically plotted according to increasing cell age (youngest cells in the top panel and oldest cells in the bottom panel). (**D**) The integral fluorescence of each cell was sorted and plotted as a function of cell length (each cell is displayed as a vertical line) using Coli-Inspector, where cell length corresponds to relative cell age (x-axis). The white horizontal line indicates midcell. A total of 523 cells were analyzed with Coli-Inspector. (**E**) The percentages of cells with zero to three SeqA (red bars) or SSB (green bars) foci per cell were plotted in a histogram. Error bars represent standard errors of the mean (SEM) of three independent experiments. A total of 423 cells were analyzed. (**F**) The distribution of SeqA-replisome distances within the three youngest age groups (replicating cells with relative ages of 0 to 0.6) was plotted in a histogram. See Figure 1F for the description of the histogram. A total of 273 cells were analyzed.

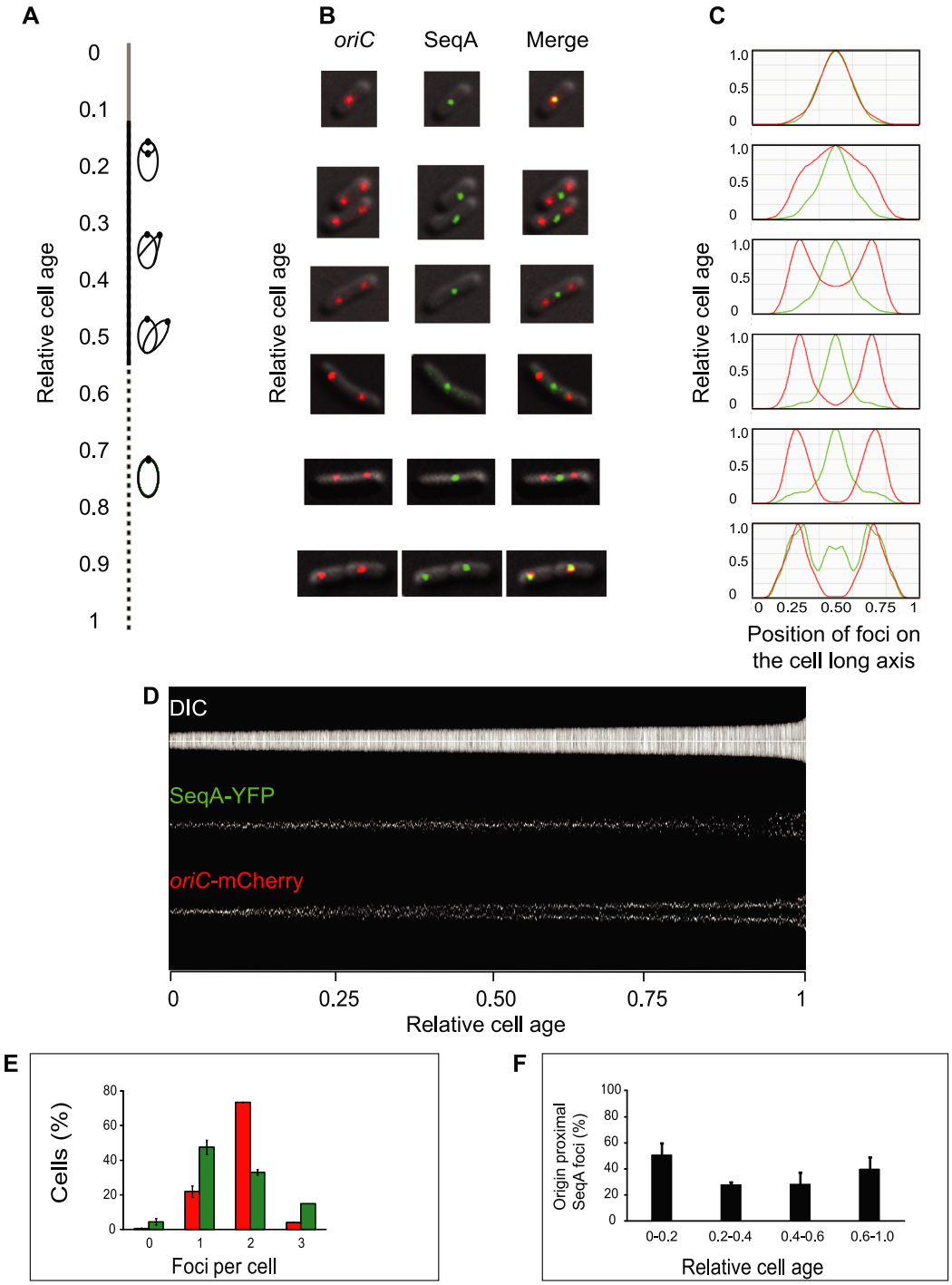

Figure 3. The SeqA protein is localized at midcell for most of the D-period, but colocalizes with the origin region before cell division and initiation of replication. (**A**) Cell cycle diagram of cells (SF148) with fluorescently tagged SeqA protein (SeqA-YFP) and origin region (FROS), grown exponentially in acetate medium with a doubling time (τ) of 250 min. See Figure 1A for the description of cell cycle diagram. The B-period is shown as a gray line. (**B**) Snapshot fluorescence imaging showed formation of discrete *oriC* (pseudo-colored red) and SeqA (pseudo-colored green) foci. Images of cells are ordered from top to bottom according to relative cell age (based on relative cell length). (**C**) Local brightness of fluorescent SeqA (green line) and *oriC* (red line) signals was plotted against foci positioning on the cell long axis (x-axis of histograms) using Coli-Inspector. The population was divided into six age groups based on relative cell length. The histograms of age groups are vertically plotted according to increasing cell age (youngest cells in the top panel and oldest cells in the bottom panel). (**D**) The integral fluorescence of each cell was sorted and plotted as a function of cell length (each cell is displayed as a vertical line) using Coli-Inspector, where cell length corresponds to relative cell age (x-axis). The white horizontal line indicates midcell. A total of 816 cells were analyzed. (**E**) The percentages of cells with zero to three SeqA (green bars) or *oriC* (red bars) foci per cell were plotted in a histogram. Error bars represent standard error of the means (SEM) of three independent experiments. A total of 591 cells were analyzed. (**F**) The percentage of SeqA and *oriC* foci that were close together (below the resolution limit) was plotted in a histogram according to four groups of increasing relative cell age (based on relative cell length). The distances that represent SeqA-origin proximal foci were normalized against the total number of distances measured for that age group. A total of 779 cells were analyzed.

origin region to each cell half. Moreover, a high percentage of old cells with SeqA at the origin region indicates that SeqA binds to the origin region prior to replication initation. This means that SeqA presumably is able to remain in multimerized complexes in the absence of hemimethylated GATC-sites and is also likely to bind to *oriC* prior to initiation.

Single-molecule localization imaging reveals that sister SeqA structures trailing a single replication fork are localized close together

We show here that the replisome and the SeqA structures are situated relatively far apart, both during rapid and slow growth. We also show that in rapidly growing cells the two SeqA structures on newly replicated sister DNA apparently could be resolved for a few cells (6%) with 3D-SIM (Supplementary Figure S6) in the period when the replication forks exhibit higher mobility (see Figure 1). This indicated that sister SeqA structures are localized closer than 120 nm (the resolution of 3D-SIM) for most of the cell cycle. However, rapidly growing cells contain substantially more DNA (and replication forks) than slowly growing cells and it may be that space restrictions force the sister SeqA structures to be localized close together. Moreover, the resolution of 3D-SIM is not high enough to discern between finely spaced foci, considering the diameter of DNA (around 2 nm). We therefore decided to (i) study the SeqA structures in slowly growing cells containing a single replicating chromosome and (ii) increase the microscopic resolution by performing dSTORM single-molecule localization imaging. The cells (AB1157) were grown at 28°C in acetate medium ($\tau = 234 \pm 17$ min) and SeqA was immunolabeled with anti-SeqA primary antibody and anti-rabbit Alexa647 secondary antibody (see the Materials and Methods section). Samples for flow cytometry were prepared as explained previously. The dSTORM fluorescence intensity information was sorted for a precision of 5–15 nm.

We categorized all the imaged cells according to relative cell length/cell cycle progression, as explained for Figures 1, 2 and 3. Figure 4A shows segmented SeqA-Alexa647 foci that are representative of cell cycle stage, in which signal captured in conventional widefield mode (pseudo-colored red) and signal captured in dSTORM mode (pseudo-colored green/yellow) are shown. The number of widefield and dSTORM foci per cell was plotted in a histogram for the replicating cell population (Figure 4B). The replicating cells were found to harbor mainly one or two midcell SeqA dSTORM foci within one widefield focus, thus representing two or one replication fork(s), respectively. A few cells (~6%) were found to contain three or four dSTORM SeqA foci at midcell (Figure 4B), which presumably indicates that two SeqA structures could be resolved for one or both of the two replication forks. The non-replicating cells contained mainly two dSTORM foci/one widefield focus at midcell or one dSTORM/widefield focus at each of the quarter positions right before cell division. The average width of dSTORM foci in replicating cells containing two foci was found to be 34 nm (focus length in both x and y directions included) (Figure 4A). Since these foci contain sister DNA strands, the result implies that SeqA structures on the sister strands were situated less than 34 nm apart in the large majority of the replicating cells.

DISCUSSION

SeqA complexes trail the replication fork at a distance whereas the SeqA complexes on the two new sister DNA molecules are situated close together

We show in this work that the SeqA structures that trail the replication forks do so at a considerable distance. We also show that the SeqA structures bound to newly replicated sister molecules are kept close to each other (Figure 5). In a few replicating cells (6%) the sister foci behind a single fork could be distinguished by dSTORM imaging. In all other cells the sister foci were located close together, and could not be resolved from fluorescence signal sorted for a precision of 5–15 nm. The fact that the sister SeqA foci could be seen apart indicates that when SeqA binds to new DNA, the structures that are built are separate on the two sister molecules.

One explanation for the large average distance between the replisome and the SeqA structure may be the difference in the size of the structures. The average frequency of GATC sites is four GATC sites every 1000 base pairs. On an *E. coli* chromosome replicating with two replication forks, each at a speed of 50 000 base pairs per min, 400–800 new GATC sites will be generated every 1–2 min. Therefore, on average 200–400 GATC sites are bound by SeqA behind each replication fork. Such a complex of several hundred SeqA molecules bound to DNA will be much larger than the replisome, and would make the DNA-bound SeqA structure relatively immobile compared to the replisome which has been reported to track along the DNA as it replicates (33).

When DNA is completely extended, 1000 base pairs will reach ~250 nm. DNA bound to nucleoid-associated proteins will, however, be much more compact. Thus it is likely that several thousand base pairs of DNA is found in between the replisome and the SeqA structure. The newest GATC sites are apparently not methylated by Dam methylase but instead incorporated into the dynamic SeqA structure. It is possible either that Dam methylase does not gain access to DNA on this side of the SeqA structure or that new GATC sites are protected either by single SeqA molecules that are recruited to the main SeqA structure as soon as the new DNA extends far enough or, alternatively, by other proteins binding to the new DNA. Only one other protein, MutH, is known to bind specifically to hemimethylated GATC sites (46). We therefore investigated whether differences in localization of the replisomes and the SeqA foci could be detected in cells lacking MutH. No differences were detected (data not shown). Thus, MutH protein does not seem to affect the localization of SeqA structures. The opposite is, however, possible, i.e. that the SeqA structure trailing the fork affects the localization of MutH and other mismatch repair proteins. We suggest that the stretch of DNA between SeqA and the replisome may be a preferred site for mismatch repair processes.

The two SeqA structures on sister DNA molecules were situated much closer together than the SeqA structure and the replisome. Thus, it could be that through parts of the cell cycle they actually exist as a common SeqA structure held

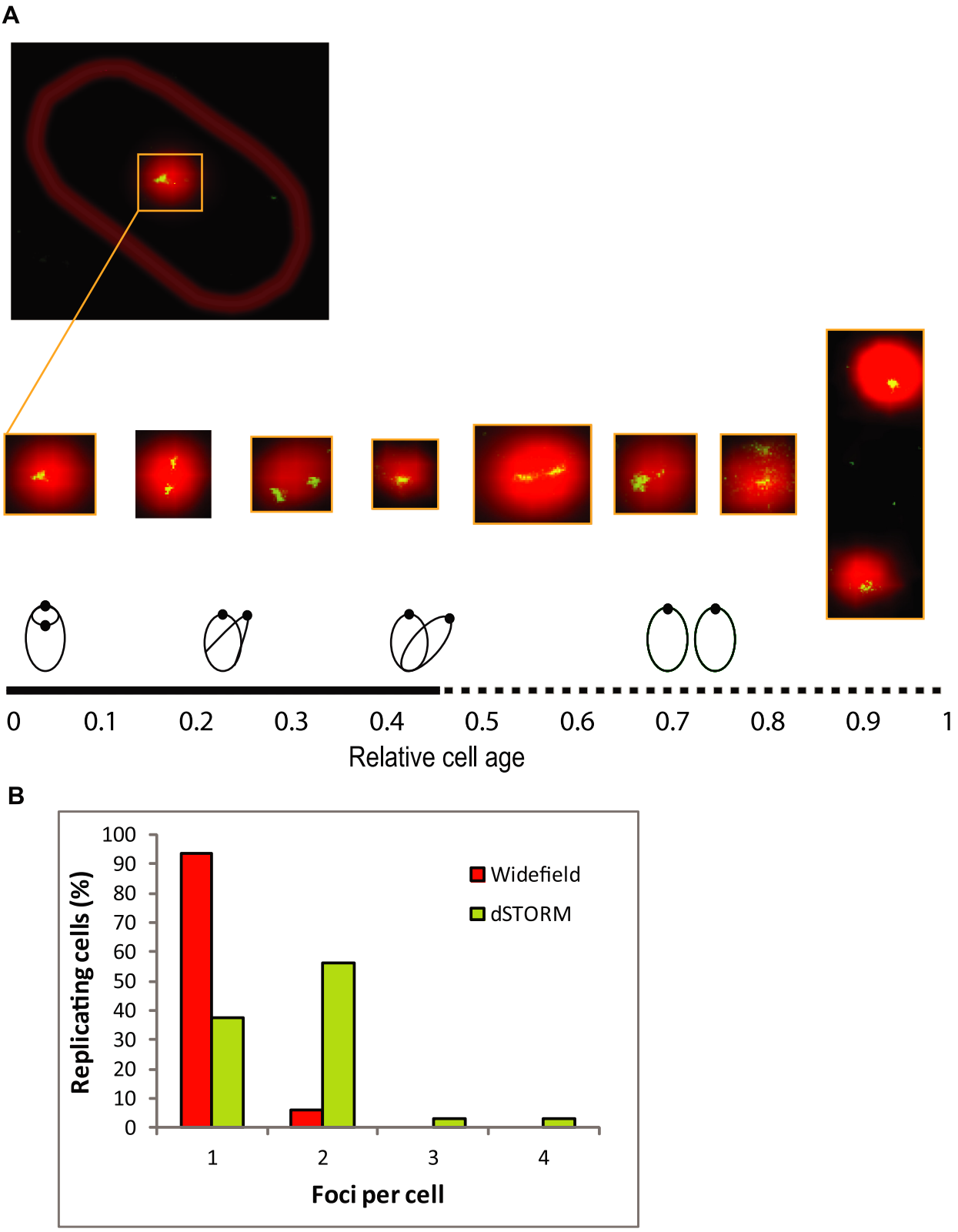

Figure 4. dSTORM imaging of immunolabeled SeqA (using secondary antibody conjugated with Alexa647) in slowly growing AB1157 cells. (**A**) Example image of a typical newborn cell where the SeqA focus is imaged in conventional widefield mode (pseudo-colored red) and in dSTORM mode (pseudo-colored green/yellow) (top panel). Segmented SeqA foci from representative cells (middle panel), arranged according to cell cycle progression (lower panel). See Figure 1A for the description of cell cycle diagram. A total of 62 cells were imaged. (**B**) Histogram showing the number of SeqA foci per cell in conventional widefield mode (red bars) and in dSTORM mode (yellow bars) in the population of replicating cells. Thirty-two cells were analyzed.

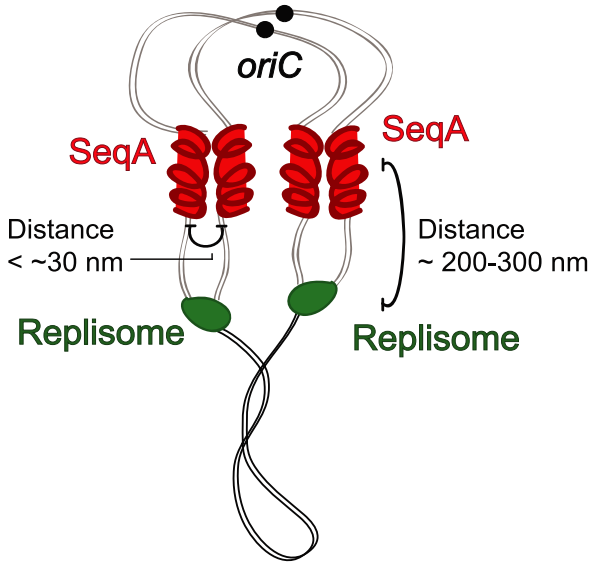

Figure 5. Model of SeqA protein trailing the replisome. Illustration of the two replication forks of one chromosome with the two replisomes included. The average distance from the replisome to the SeqA structures of the same replication fork and the maximum distance between the SeqA structures on the two daughter molecules are indicated. Unreplicated DNA in black, new DNA in gray, replisomes in green, *oriC* as black dots and SeqA in red.

together by SeqA–SeqA interactions. *In vitro* experiments show that SeqA structures formed on newly replicated DNA are capable of holding the two daughter molecules together (15). Alternatively, two separate SeqA structures could be held together by other means, for instance other proteins. The only protein so far known to possibly interact with SeqA is ParC, a subunit of Topoisomerase IV (TopoIV) (25). As a replication fork moves forward, topological stress increases in front of the fork. Most of this stress is removed by the action of DNA gyrase (47). In addition, some of this stress may be relieved by rotation of the replisome. This will transfer positive supercoils in front of the fork into precatenanes behind the fork (48–50). TopoIV has been suggested to play a role in removal of the precatenanes behind the replication forks (51) and SeqA has been suggested to modulate this process (24). An interaction between ParC and SeqA might hold the separate SeqA structures on daughter strands together. It is also possible that two such SeqA structures may be held together not by a protein but by the formation of the precatenanes. The large SeqA structure would in such a case possibly function as a barrier to further diffusion of the precatenanes and would create a defined stretch of DNA on which TopoIV could act.

In acetate grown cells the distance between the replisome and the SeqA structure was at its largest in cells where the replisomes had moved out to the quarter positions while the SeqA focus was situated at midcell, giving the impression that the SeqA structure was held back at midcell. It is thus possible that not only the two sister SeqA structures are held actively together but also the four SeqA structures belonging to pairs of forks. It is so far not clear whether the midcell SeqA structures contain the origin regions, i.e. whether origins are still in sequestration.

It has been suggested that SeqA binding helps direct the newly synthesized sister molecules away from the forks and away from each other (20). The opposite scenario has also been suggested, namely that the SeqA structures constitute spacers between replication forks and segregation forces and that this prevents segregation from destabilizing the replication forks (21,22). The present results support the idea that newly replicated sister molecules are kept together behind the fork. However, it is only in the slowly growing cells that a possible problem with segregation would be an issue because in rapidly growing cells with multifork replication, newly replicated sister DNA molecules co-segregate (30) and stay colocalized for large parts of the cell cycle (15). Since rapidly growing cells suffer more than slowly growing cells upon loss of SeqA activity it is reasonable to assume that a possible prevention of the 'segregation fork' from reaching the replication fork is not the main function of SeqA. We suggest that the newly replicated sister DNA molecules in between the replisome and the two sister SeqA structures enjoy added stabilization. This stabilization, and the fact that homologous DNA then exists nearby, may be important for DNA recombination and repair processes.

SeqA foci are observed in cells that do not contain newly replicated DNA

SeqA was found to be located at midcell in the D-period of slowly growing cells, before relocalizing to the origin regions at the end of the cell cycle (Figures 3 and 4). The result was surprising because SeqA is known to bind to either fully methylated *oriC* or to hemimethylated GATC sites following the replication fork. Since D-period cells do not contain replication forks it is likely that there is no hemimethylated DNA present either. Thus, it is not clear whether SeqA is bound to DNA when situated at midcell in D-period cells. It is possible that hemimethylated GATC sites in the Ter region with SeqA protein bound persist when replication forks terminate because new sites are no longer generated. However, the Ter region contains few GATC sites. During rapid growth very little SeqA is bound to the terminus parts of the chromosome (18) and the Ter region does not colocalize with SeqA foci (30). Most of the SeqA in rapidly growing cells is found in structures containing hemimethylated DNA trailing the newest forks of the multifork chromosomes. Thus, in the slowly growing cells it could well be that the midcell SeqA structure does not contain DNA. If so, the result may indicate that the SeqA structures are built in such a way that DNA can escape easily and that binding to DNA is not required to keep the SeqA structures intact. Thus, it may simply be that DNA escapes from the SeqA structure, and that the SeqA proteins remain in the oligomerized state. So far we do not understand what role(s) SeqA may have at this stage in the cell cycle. It is also not known what causes SeqA to cease being an oligomer at midcell and instead binds to the fully methylated origins.

SeqA binds to the origin region prior to initiation of replication

It has previously been found that SeqA binds preferentially to two or more hemimethylated GATC sites, but also

to fully methylated *oriC* (with lower affinity) (7). Here we present results that indicate SeqA binding to the origin region as early as ∼45 min before cell division and 70 min before replication initiation in slowly growing cells, at times where *oriC* is fully methylated (Figures 3 and 4).

For initiation of replication to occur, DnaA must recognize specific sequences (*dnaA* boxes) in the *oriC* region and form an orisome complex (52–56). However, in the initiation process not only the sequence specificity of the *dnaA* boxes and binding of DnaA but also the topology of the DNA has been shown to be important (57–63). For example, it is known that negative supercoiling of the DNA in *oriC* promotes DNA unwinding (64). Also, loop formation within an unstable region in *oriC* has been suggested to initiate DNA unwinding and enable interaction between distantly separated oligomers of DnaA (53,60,62,65). Nucleoid-associated proteins such as Fis, IHF and HU have been proposed to modulate *oriC* topology for regulation of replication initiation (in addition to DnaA) (57,62,63,66–68), but in this context the role of SeqA remains to be explored. A positive effect of SeqA on initiation has been found at low DnaA concentrations *in vitro* (69). However, *in vivo* work strongly indicates that SeqA is mainly a negative regulator of replication initiation (70).

In our studies the SeqA foci colocalized with the origin regions prior to replication initiation are likely to consist of oligomerized higher-order forms of SeqA. Such complexes would presumably present steric challenges for DnaA binding, and possibly also restrain negative supercoils in the DNA (11). Also, the organization of DNA into SeqA-*oriC* complexes may change the distribution of DnaA protein at the binding sites, as proposed by Wold *et al.* in 1998 (69). So far there has been no evidence of a positive role of SeqA in replication initiation *in vivo*, and it has been found that SeqA null mutants initiate replication on average at 10–20% lower mass compared to wild-type cells in poor medium (70). This premature initiation was not due to increased levels of DnaA (DnaA levels were similar to in wild-type cells) (70). Thus, it is likely that SeqA has a role as a negative regulator at fully methylated origins in addition to its role in sequestration of recently initiated, hemimethylated origins. It is possible that this role is different in poor medium where initiation of replication occurs with no hemimethylated DNA present elsewhere on the chromosome, compared to in rich medium where replication forks and hemimethylated GATC sites are always present.

SUPPLEMENTARY DATA

Supplementary Data are available at NAR Online.

ACKNOWLEDGEMENTS

We thank A. Wahl for excellent technical assistance and I. Flåtten for critical reading of the manuscript. The Flow Cytometry Core Facility (by T. Stokke and K. Landsverk) and the Super-resolution Core Facility (E. Skarpen/V. Sørensen) at The Norwegian Radium Hospital are greatly acknowledged for help with flow cytometry analysis and super-resolution microscopy (3D-SIM and dSTORM), respectively. We thank M. Radman, A. Wright, R. Reyes-Lamothe and D.J. Sherratt for providing strains.

FUNDING

MLS (EMBIO) at University of Oslo [to S.F.R.]; the Research Council of Norway [to E.H.]. Funding for open access charge: Oslo University Hospital.
Conflict of interest statement. None declared.

REFERENCES

1. Cooper,S. and Helmstetter,C.E. (1968) Chromosome replication and the division cycle of *Escherichia coli* B/r. *J. Mol. Biol.*, **31**, 519–540.
2. Dorman,C.J. (2013) Genome architecture and global gene regulation in bacteria: making progress towards a unified model? *Nat. Rev. Microbiol.*, **11**, 349–355.
3. Lu,M., Campbell,J.L., Boye,E. and Kleckner,N. (1994) SeqA: a negative modulator of replication initiation in E. coli. *Cell*, **77**, 413–426.
4. von Freiesleben,U., Rasmussen,K.V. and Schaechter,M. (1994) SeqA limits DnaA activity in replication from *oriC* in *Escherichia coli*. *Mol. Microbiol.*, **14**, 763–772.
5. Campbell,J.L. and Kleckner,N. (1990) *E. coli oriC* and the dnaA gene promoter are sequestered from dam methyltransferase following the passage of the chromosomal replication fork. *Cell*, **62**, 967–979.
6. Brendler,T. and Austin,S. (1999) Binding of SeqA protein to DNA requires interaction between two or more complexes bound to separate hemimethylated GATC sequences. *EMBO J.*, **18**, 2304–2310.
7. Slater,S., Wold,S., Lu,M., Boye,E., Skarstad,K. and Kleckner,N. (1995) *E. coli* SeqA protein binds *oriC* in two different methyl-modulated reactions appropriate to its roles in DNA replication initiation and origin sequestration. *Cell*, **82**, 927–936.
8. Han,J.S., Kang,S., Lee,H., Kim,H.K. and Hwang,D.S. (2003) Sequential binding of SeqA to paired hemi-methylated GATC sequences mediates formation of higher order complexes. *J. Biol. Chem.*, **278**, 34983–34989.
9. Torheim,N.K. and Skarstad,K. (1999) *Escherichia coli* SeqA protein affects DNA topology and inhibits open complex formation at *oriC*. *EMBO J.*, **18**, 4882–4888.
10. Klungsoyr,H.K. and Skarstad,K. (2004) Positive supercoiling is generated in the presence of *Escherichia coli* SeqA protein. *Mol. Microbiol.*, **54**, 123–131.
11. Odsbu,I., Klungsoyr,H.K., Fossum,S. and Skarstad,K. (2005) Specific N-terminal interactions of the *Escherichia coli* SeqA protein are required to form multimers that restrain negative supercoils and form foci. *Genes Cells*, **10**, 1039–1049.
12. Guarne,A., Brendler,T., Zhao,Q., Ghirlando,R., Austin,S. and Yang,W. (2005) Crystal structure of a SeqA-N filament: implications for DNA replication and chromosome organization. *EMBO J.*, **24**, 1502–1511.
13. Molina,F. and Skarstad,K. (2004) Replication fork and SeqA focus distributions in *Escherichia coli* suggest a replication hyperstructure dependent on nucleotide metabolism. *Mol. Microbiol.*, **52**, 1597–1612.
14. Adachi,S., Kohiyama,M., Onogi,T. and Hiraga,S. (2005) Localization of replication forks in wild-type and mukB mutant cells of *Escherichia coli*. *Mol. Genet. Genomics*, **274**, 264–271.
15. Fossum,S., Crooke,E. and Skarstad,K. (2007) Organization of sister origins and replisomes during multifork DNA replication in *Escherichia coli*. *EMBO J.*, **26**, 4514–4522.
16. Morigen Odsbu,I. and Skarstad,K. (2009) Growth rate dependent numbers of SeqA structures organize the multiple replication forks in rapidly growing *Escherichia coli*. *Genes Cells*, **14**, 643–657.
17. Waldminghaus,T. and Skarstad,K. (2009) The *Escherichia coli* SeqA protein. *Plasmid*, **61**, 141–150.
18. Waldminghaus,T., Weigel,C. and Skarstad,K. (2012) Replication fork movement and methylation govern SeqA binding to the *Escherichia coli* chromosome. *Nucleic Acids Res.*, **40**, 5465–5476.
19. Cagliero,C., Grand,R.S., Jones,M.B., Jin,D.J. and O'Sullivan,J.M. (2013) Genome conformation capture reveals that the *Escherichia coli* chromosome is organized by replication and transcription. *Nucleic Acids Res.*, **41**, 6058–6071.

20. Brendler,T., Sawitzke,J., Sergueev,K. and Austin,S. (2000) A case for sliding SeqA tracts at anchored replication forks during *Escherichia coli* chromosome replication and segregation. *EMBO J.*, **19**, 6249–6258.
21. Kuzminov,A. (2013) The chromosome cycle of prokaryotes. *Mol. Microbiol.*, **90**, 214–227.
22. Rotman,E., Khan,S.R., Kouzminova,E. and Kuzminov,A. (2014) Replication fork inhibition in seqA mutants of *Escherichia coli* triggers replication fork breakage. *Mol. Microbiol.*, **93**, 50–64.
23. Kouzminova,E.A., Rotman,E., Macomber,L., Zhang,J. and Kuzminov,A. (2004) RecA-dependent mutants in *Escherichia coli* reveal strategies to avoid chromosomal fragmentation. *Proc. Natl. Acad. Sci. U.S.A.*, **101**, 16262–16267.
24. Joshi,M.C., Magnan,D., Montminy,T.P., Lies,M., Stepankiw,N. and Bates,D. (2013) Regulation of sister chromosome cohesion by the replication fork tracking protein SeqA. *PLoS Genet.*, **9**, e1003673.
25. Kang,S., Han,J.S., Park,J.H., Skarstad,K. and Hwang,D.S. (2003) SeqA protein stimulates the relaxing and decatenating activities of topoisomerase IV. *J. Biol. Chem.*, **278**, 48779–48785.
26. Howard-Flanders,P., Simon,E. and Theriot,L. (1964) A locus that controls filament formation and sensitivity to radiation in *Escherichia coli* K-12. *Genetics*, **49**, 237–246.
27. Lindner,A.B., Madden,R., Demarez,A., Stewart,E.J. and Taddei,F. (2008) Asymmetric segregation of protein aggregates is associated with cellular aging and rejuvenation. *Proc. Natl. Acad. Sci. U.S.A.*, **105**, 3076–3081.
28. Babic,A., Lindner,A.B., Vulic,M., Stewart,E.J. and Radman,M. (2008) Direct visualization of horizontal gene transfer. *Science*, **319**, 1533–1536.
29. Miller,J.H. (1992) *A Short Course in Bacterial Genetics*. Cold Spring Harbor Laboratory Press, Cold Spring Harbor, NY.
30. Fossum-Raunehaug,S., Helgesen,E., Stokke,C. and Skarstad,K. (2014) *Escherichia coli* SeqA structures relocalize abruptly upon termination of origin sequestration during multifork DNA replication. *PLoS ONE*, **9**, e110575.
31. Lau,I.F., Filipe,S.R., Soballe,B., Okstad,O.A., Barre,F.X. and Sherratt,D.J. (2003) Spatial and temporal organization of replicating *Escherichia coli* chromosomes. *Mol. Microbiol.*, **49**, 731–743.
32. Possoz,C., Filipe,S.R., Grainge,I. and Sherratt,D.J. (2006) Tracking of controlled *Escherichia coli* replication fork stalling and restart at repressor-bound DNA *in vivo*. *EMBO J.*, **25**, 2596–2604.
33. Reyes-Lamothe,R., Possoz,C., Danilova,O. and Sherratt,D.J. (2008) Independent positioning and action of *Escherichia coli* replisomes in live cells. *Cell*, **133**, 90–102.
34. Datsenko,K.A. and Wanner,B.L. (2000) One-step inactivation of chromosomal genes in *Escherichia coli* K-12 using PCR products. *Proc. Natl. Acad. Sci. U.S.A.*, **97**, 6640–6645.
35. Clark,D.J. and Maaløe,O. (1967) DNA replication and division cycle in *Escherichia coli*. *J. Mol. Biol.*, **23**, 99–112.
36. Skarstad,K., Boye,E. and Steen,H.B. (1986) Timing of initiation of chromosome replication in individual *Escherichia coli* cells. *EMBO J.*, **5**, 1711–1717.
37. Boye,E. and Løbner-Olesen,A. (1991) Bacterial growth control studied by flow cytometry. *Res. Microbiol.*, **142**, 131–135.
38. Flatten,I., Morigen, and Skarstad,K. (2009) DnaA protein interacts with RNA polymerase and partially protects it from the effect of rifampicin. *Mol. Microbiol.*, **71**, 1018–1030.
39. Torheim,N.K., Boye,E., Løbner-Olesen,A., Stokke,T. and Skarstad,K. (2000) The *Escherichia coli* SeqA protein destabilizes mutant DnaA204 protein. *Mol. Microbiol.*, **37**, 629–638.
40. Stokke,C., Flatten,I. and Skarstad,K. (2012) An easy-to-use simulation program demonstrates variations in bacterial cell cycle parameters depending on medium and temperature. *PLoS. ONE*, **7**, e30981.
41. Fossum,S., Soreide,S. and Skarstad,K. (2003) Lack of SeqA focus formation, specific DNA binding and proper protein multimerization in the *Escherichia coli* sequestration mutant seqA2. *Mol. Microbiol.*, **47**, 619–632.
42. Huang,F., Hartwich,T.M.P., Rivera-Molina,F.E., Lin,Y., Duim,W.C., Long,J.J., Uchil,P.D., Myers,J.R., Baird,M.A., Mothes,W. *et al.* (2013) Video-rate nanoscopy using sCMOS camera-specific single-molecule localization algorithms. *Nat. Methods*, **10**, 653–658.
43. Potluri,L., Karczmarek,A., Verheul,J., Piette,A., Wilkin,J.M., Werth,N., Banzhaf,M., Vollmer,W., Young,K.D., Nguyen-Disteche,M. *et al.* (2010) Septal and lateral wall localization of PBP5, the major D, D-carboxypeptidase of *Escherichia coli*, requires substrate recognition and membrane attachment. *Mol. Microbiol.*, **77**, 300–323.
44. Geier,G.E. and Modrich,P. (1979) Recognition sequence of the dam methylase of *Escherichia coli* K12 and mode of cleavage of Dpn I endonuclease. *J. Biol. Chem.*, **254**, 1408–1413.
45. Brendler,T., Abeles,A. and Austin,S. (1995) A protein that binds to the P1 origin core and the *oriC* 13mer region in a methylation-specific fashion is the product of the host seqA gene. *EMBO J.*, **14**, 4083–4089.
46. Langle-Rouault,F., Maenhaut-Michel,G. and Radman,M. (1987) GATC sequences, DNA nicks and the MutH function in *Escherichia coli* mismatch repair. *EMBO J.*, **6**, 1121–1127.
47. Khodursky,A.B. and Cozzarelli,N.R. (1998) The mechanism of inhibition of topoisomerase IV by quinolone antibacterials. *J. Biol. Chem.*, **273**, 27668–27677.
48. Espeli,O. and Marians,K.J. (2004) Untangling intracellular DNA topology. *Mol. Microbiol.*, **52**, 925–931.
49. Schvartzman,J.B. and Stasiak,A. (2004) A topological view of the replicon. *EMBO Rep.*, **5**, 256–261.
50. Postow,L., Hardy,C.D., Arsuaga,J. and Cozzarelli,N.R. (2004) Topological domain structure of the *Escherichia coli* chromosome. *Genes Dev.*, **18**, 1766–1779.
51. Wang,X., Reyes-Lamothe,R. and Sherratt,D.J. (2008) Modulation of *Escherichia coli* sister chromosome cohesion by topoisomerase IV. *Genes Dev.*, **22**, 2426–2433.
52. Fuller,R.S., Funnell,B.E. and Kornberg,A. (1984) The dnaA protein complex with the *E. coli* chromosomal replication origin (oriC) and other DNA sites. *Cell*, **38**, 889–900.
53. Speck,C. and Messer,W. (2001) Mechanism of origin unwinding: sequential binding of DnaA to double- and single-stranded DNA. *EMBO J.*, **20**, 1469–1476.
54. McGarry,K.C., Ryan,V.T., Grimwade,J.E. and Leonard,A.C. (2004) Two discriminatory binding sites in the *Escherichia coli* replication origin are required for DNA strand opening by initiator DnaA-ATP. *Proc. Natl. Acad. Sci. U.S.A.*, **101**, 2811–2816.
55. Ozaki,S., Kawakami,H., Nakamura,K., Fujikawa,N., Kagawa,W., Park,S.Y., Yokoyama,S., Kurumizaka,H. and Katayama,T. (2008) A common mechanism for the ATP-DnaA-dependent formation of open complexes at the replication origin. *J. Biol. Chem.*, **283**, 8351–8362.
56. Ozaki,S. and Katayama,T. (2009) DnaA structure, function, and dynamics in the initiation at the chromosomal origin. *Plasmid*, **62**, 71–82.
57. Ryan,V.T., Grimwade,J.E., Camara,J.E., Crooke,E. and Leonard,A.C. (2004) *Escherichia coli* prereplication complex assembly is regulated by dynamic interplay among Fis, IHF and DnaA. *Mol. Microbiol.*, **51**, 1347–1359.
58. Skarstad,K., Baker,T.A. and Kornberg,A. (1990) Strand separation required for initiation of replication at the chromosomal origin of *E.coli* is facilitated by a distant RNA–DNA hybrid. *EMBO J.*, **9**, 2341–2348.
59. Baker,T.A., Sekimizu,K., Funnell,B.E. and Kornberg,A. (1986) Extensive unwinding of the plasmid template during staged enzymatic initiation of DNA replication from the origin of the *Escherichia coli* chromosome. *Cell*, **45**, 53–64.
60. Ozaki,S. and Katayama,T. (2012) Highly organized DnaA-oriC complexes recruit the single-stranded DNA for replication initiation. *Nucleic Acids Res.*, **40**, 1648–1665.
61. Donczew,R., Weigel,C., Lurz,R., Zakrzewska-Czerwinska,J. and Zawilak-Pawlik,A. (2012) Helicobacter pylori *oriC*–the first bipartite origin of chromosome replication in Gram-negative bacteria. *Nucleic Acids Res.*, **40**, 9647–9660.
62. Kaur,G., Vora,M.P., Czerwonka,C.A., Rozgaja,T.A., Grimwade,J.E. and Leonard,A.C. (2014) Building the bacterial orisome: high-affinity DnaA recognition plays a role in setting the conformation of *oriC* DNA. *Mol. Microbiol.*, **91**, 1148–1163.
63. Donczew,R., Zakrzewska-Czerwinska,J. and Zawilak-Pawlik,A. (2014) Beyond DnaA: the role of DNA topology and DNA methylation in bacterial replication initiation. *J. Mol. Biol.*, **426**, 2269–2282.
64. Kataoka,T., Wachi,M., Nakamura,J., Gayama,S., Yamasaki,M. and Nagai,K. (1993) Fully methylated *oriC* with negative superhelicity

forms an oriC-membrane complex before initiation of chromosome replication. *Biochem. Biophys. Res. Commun.*, **194**, 1420–1426.
65. Ozaki,S., Noguchi,Y., Hayashi,Y., Miyazaki,E. and Katayama,T. (2012) Differentiation of the DnaA-*oriC* subcomplex for DNA unwinding in a replication initiation complex. *J. Biol. Chem.*, **287**, 37458–37471.
66. Ryan,V.T., Grimwade,J.E., Nievera,C.J. and Leonard,A.C. (2002) IHF and HU stimulate assembly of pre-replication complexes at *Escherichia coli* oriC by two different mechanisms. *Mol. Microbiol.*, **46**, 113–124.
67. von Freiesleben,U., Rasmussen,K.V., Atlung,T. and Hansen,F.G. (2000) Rifampicin-resistant initiation of chromosome replication from *oriC* in ihf mutants. *Mol. Microbiol.*, **37**, 1087–1093.
68. Flatten,I. and Skarstad,K. (2013) The Fis protein has a stimulating role in initiation of replication in *Escherichia coli* in vivo. *PLoS ONE*, **8**, e83562.
69. Wold,S., Boye,E., Slater,S., Kleckner,N. and Skarstad,K. (1998) Effects of purified SeqA protein on *oriC*-dependent DNA replication *in vitro*. *EMBO J.*, **17**, 4158–4165.
70. Boye,E., Stokke,T., Kleckner,N. and Skarstad,K. (1996) Coordinating DNA replication initiation with cell growth: differential roles for DnaA and SeqA proteins. *Proc. Natl. Acad. Sci. U.S.A.*, **93**, 12206–12211.